Baghdad Science Journal

Volume 22 | Issue 2 Article 11

2025

Synthesis Characterization and Adsorption of Doxorubicin Hydrochloride on SiO2 Nanoparticle for Drug Delivery

Asmaa H. Hammadi
Department of Pharmaceuticals, College of Pharmacy, University of Babylon, Hilla, Iraq,
ashashim4@gmail.com

Noor Hadi Aysa
Department of Clinical and Laboratory Sciences, College of Pharmacy, University of Babylon, Hilla, Iraq,
noorpharmacy83@gmail.com

Fattima Al-Zahra Gabar Gassim
Department of Pharmaceuticals, College of Pharmacy, University of Babylon, Hilla, Iraq,
alzahraafatema6@gmail.com

How to Cite this Article

Hammadi, Asmaa H.; Aysa, Noor Hadi; and Gabar Gassim, Fattima Al-Zahra (2025) "Synthesis Characterization and Adsorption of Doxorubicin Hydrochloride on SiO2 Nanoparticle for Drug Delivery," *Baghdad Science Journal*: Vol. 22: Iss. 2, Article 11.
DOI: https://doi.org/10.21123/bsj.2024.10048

BAGHDAD SCIENCE JOURNAL 2025;22(2):472–485

Scan the QR to view the full-text article on the journal website

RESEARCH ARTICLE

Synthesis Characterization and Adsorption of Doxorubicin Hydrochloride on SiO_2 Nanoparticle for Drug Delivery

Asmaa H. Hammadi [1,*], **Noor Hadi Aysa** [2], **Fattima Al-Zahra Gabar Gassim** [1]

[1] Department of Pharmaceuticals, College of Pharmacy, University of Babylon, Hilla, Iraq
[2] Department of Clinical and Laboratory Sciences, College of Pharmacy, University of Babylon, Hilla, Iraq

ABSTRACT

In the present study, Tetraethyl orthosilicate (TEOS), polyethylene glycol 5%, and HCl 0.001 N are used to chemically create silica nanoparticles (SiO_2 NPs). The manufacturing of nano silica-gel doxorubicin (DOX) loaded silica nanoparticles (DOX/SiO_2), which is commonly applied as part of the drug delivery systems in cancer therapy, was done using the sol-gel method. The morphology and surface content of the produced DOX/silica loaded nanoparticles were studied using different techniques including the X-ray diffraction (XRD), Scanning Electron Microscopy (SEM), and the Fourier Transform Infra-Red (FTIR) spectroscopy spectrum. The synthesized DOX/SiO_2 has a diameter of 38 nm. The isothermal adsorption follows the Freundlich isotherm and the adsorption kinetics fit to the pseudo-second order. The R2 values for the Freundlich and Langmuir models were 0.9931 and 0.9731, respectively, showing that the Freundlich isotherm tends to be more suitable with the experimental data as compared to the Langmuir model. This study aims at using nanotechnology in drug delivery. A drug delivery system is characterized as a formulation or a device that facilitates the delivery of a medicinal substance into the body, enhancing its safety and efficacy through the regulation of the rate, time, and site of drug release into the body.

Keywords: Adsorption, Doxorubicin, Drug delivery, SiO_2 nanoparticle, Sol gol method

Introduction

It has been commonly agreed upon that cancer represents one of the worst diseases in the world. Millions of people are still living with cancer today, with colorectal cancer being among the most often diagnosed types of cancer and the primary cause of fatalities in cancer diagnoses. [1]

One of the most effective chemotherapeutic antitumor medications for treating various solid malignant tumors is the anthracycline antibiotic doxorubicin (DOX). The DOX is made up of planar anthraquinone nuclei connected to amino sugars by a glycosidic link. [2] The sugar amino groups are protonated through the generation of DOX hydrochloride for promoting aqueous solubility (DOX-HCl). Given the hydrophilicity of the sugar portion within the molecule, the flat anthraquinone portion is of high lipophilicity. The amino sugar in the DOX-HCl molecule contains a number of functional groups, including phenolic rings, acids, and bases. The DOX-HCl molecule is a result of its amphiphilic and amphoteric nature. [3] Its practical applications, however, have been constrained by severe side effects such cardiomyopathy and congestive heart failure. [4,5]

The properties of the object were enhanced by lowering potential toxicity. The creation of efficient techniques of targeted medicine delivery is crucial to reducing potential toxicities and enhancing its qualities. [6]

Drug delivery systems, such as nanoparticle-based ones using polymers, gold nanoparticles, and

Received 27 October 2023; revised 18 May 2024; accepted 20 May 2024.
Available online 21 February 2025

* Corresponding author.
E-mail addresses: ashashim4@gmail.com (A. H. Hammadi), noorpharmacy83@gmail.com (N. H. Aysa), alzahraafatema6@gmail.com (F. A.-Z. Gabar Gassim).

https://doi.org/10.21123/bsj.2024.10048

micelles have become of interest to cancer-related nanomedicine in recent years, being the carrier for loading and distributing medications for cancer therapy.[7]

The optimum cancer chemotherapy, in general, calls for both adequate drug loading and targeted drug delivery to the cancer site with minimal redundant drug buildup in the normal tissues. This can be done by selecting the best compositions and carefully adjusting the features of the resulting drug delivery system.[8,9]

Due to their good drug loading capacity, simplicity in production and modification, minimal cytotoxicity, and great biocompatibility, silica nanoparticles are thought to be one of the most commonly used materials.[10,11] Various types of silica nanoparticles with versatile properties have been developed as drug delivery systems which have achieved significant success. These silica nanoparticles have versatile surfaces that can be modified with functional groups via chemical reaction and/or physical absorption.[12–14]

Magnetic nanoparticles offer a considerable potential for tailored drug administration, as silica surface changes help them in avoiding agglomeration, increasing stability, and creating connections to other functional groups. However, the restricted amount of functional groups present on nanoparticle surfaces decreases how efficient its drug loading is, typically below 20%. The limited effectiveness of drug loading requires a lot of nanoparticle carriers to be used. This could cause the nanoparticle carrier to become poisonous, biodegradable, or metabolized among other issues.[6,15,16]

Mesoporous silica (SiO_2) nanoparticles offer a number of benefits, such as large specific surface areas, superior biocompatibility, porous architectures, and surfaces that can be modified. The most widely used NPs, SiO_2, are being thoroughly studied for use in biomedicine. At astonishing rates, research and development have been conducted on their possible uses for medication delivery.[17] The primary components of SiO_2 NPs are siloxane groups, which, following drug delivery, can be hydrolyzed to produce orthosilicic acid in the human body. These goods are easily eliminated by the urine system and are biocompatible. Due to the high stability of silica in biological environments, the primary benefits of silica nanostructures in biological applications are their ability to function as protective layers or as vehicles for drug delivery. The exceptional biocompatibility and lack of cytotoxicity of the silica shells greatly increase the stability of the protected compounds in the cores. Positively charged medications can be readily absorbed onto SiO_2 NPs pores and surfaces by strong electrostatic contact because of the silanol groups (Si-OH) on these surfaces, which confer a significantly negative zeta potential. More significantly, by understanding this mechanism, one may regulate the drug's release at the targets.[18,19] Lastly, it's important to note that silica shells have the ability to change the optical characteristics of the dye molecules they contain in this case, DOX. One of the most widely utilized antitumor medications is doxorubicin (DOX), a broad spectrum anticancer agent used in treatment for hematological malignancies and solid tumors. The development of efficient treatment strategies for targeted drug administration is essential to reducing potential toxicities and improving its characteristics.[8,20,21]

The drug doxorubicin (DOX) was incorporated into nanoparticles to showcase its possible use in the delivery of tiny molecules. After SiO_2 NPs were formed, the optical characteristics of both the free DOX molecule and the adsorbed DOX NPs were examined. Absorption spectra were used to track the drug loading efficiency.[22] The outcomes demonstrated that electrostatic interaction successfully loaded approximately 98% of DOX onto the surface of SiO_2 NPs. Depending on the solution's pH, the DOX release from these NPs. These findings demonstrate the efficacy of the DOX_HCl-SiO_2 NPs system as a drug delivery system and its considerable potential for clinical use.[19,23]

The goal of this study was to optimize DOX loading into the carrier in order to reduce waste during the drug loading phase. The prepared SiO_2 and DOX-loaded SiO_2 are characterized through various techniques such as scanning electron microscopy (SEM), X-ray diffraction (XRD), and Fourier transform infrared (FTIR) spectroscopy spectrum. The adsorption efficiency of DOX on SiO_2 is compared at different parameters, and the corresponding isotherms, kinetics, and thermodynamic parameters of DOX adsorption onto SiO_2 are studied. Finally, a plausible adsorption mechanism is proposed.

Materials and methods

The Doxorubicin Hydrochloride (99.1%) was collected from Hyper Chem, China, Tetraethyl orthosilicate (TEOS) (99%) from Germany and Poly-Ethylene Glycol (PEG) (98) from USA.

Synthesis of SiO_2 NPs

Tetraethyl orthosilicate (TEOS) is used as a precursor material for the hydrolysis and condensation of pure nano silica gel. The process typically starts with the selection of silicon alkoxide precursors, such as tetraethyl orthosilicate (TEOS) or tetramethyl orthosilicate (TMOS). TEOS is a commonly used silica

precursor in the sol-gel method.[24] It contains silicon and can undergo hydrolysis and condensation reactions to form silica nanoparticles. The chosen precursor undergoes hydrolysis in the presence of water and a catalyst, leading to the formation of silanol groups.

The process is created using TEOS and 5% Poly-Ethylene Glycol (PEG) and 0.001 N hydrochloric acid (HCl). PEG is a polymer with excellent solubility in water and is often used in nanoparticle synthesis for several reasons; PEG can act as a stabilizing agent, preventing the agglomeration of nanoparticles during synthesis, can influence the size and morphology of nanoparticles. It is biocompatible, making it suitable for applications in drug delivery or other biomedical fields. The specific concentration of PEG (5%) has been chosen to achieve a balance between stabilization and control over particle size. The concentration of PEG can impact the size and stability of the resulting nanoparticles. The combination of TEOS with PEG can influence the properties of the resulting SiO_2 nanoparticles. PEG may also serve as a template or structure-directing agent, affecting the final morphology of the nanoparticles.[25] An amount of (80 g) of PEG was mixed with 5g of TEOS (solution 1). A clouded solution was created by adding (30 ml) of HCl 0.001 N to solution 1 drop-by-drop over the course of 10 minutes while stirring at a speed of 250 rpm. The addition of 0.001 N HCl allows the researcher to control and fine-tune the pH, ensuring the stability of the sol and preventing premature gelation. The resulting solution was agitated at 250 rpm. Next, the pH was being tested. At a pH of around 2, (10 ml) of HCl 0.1 N was added instantly.[8,9] Setting a viscous gel at 80 °C allows for controlled kinetics of hydrolysis and condensation reactions. This temperature might be suitable for achieving a stable gel state before proceeding to subsequent processing steps. The gelation step is critical for determining the pore structure and particle size of the final SiO_2 nanoparticles. A controlled and viscous gel state at 80 °C can contribute to uniform particle size and porous structure.[26] The produced samples were heated for three hours at temperatures between 200 and 1000 °C. The heating process at temperatures between 200 and 1000 °C likely involves the removal of solvents and organic components from the gel. This step is essential for obtaining a porous and stable SiO_2 structure. Crystallization and Phase Transformation: The heating process promotes crystallization and phase transformation of the amorphous silica gel to form well-defined SiO_2 nanoparticles. The specific range of temperatures (200 to 1000 °C) may correspond to different stages of this transformation, influencing the final properties of the nanoparticles. The duration of three hours allows for controlled calcination,

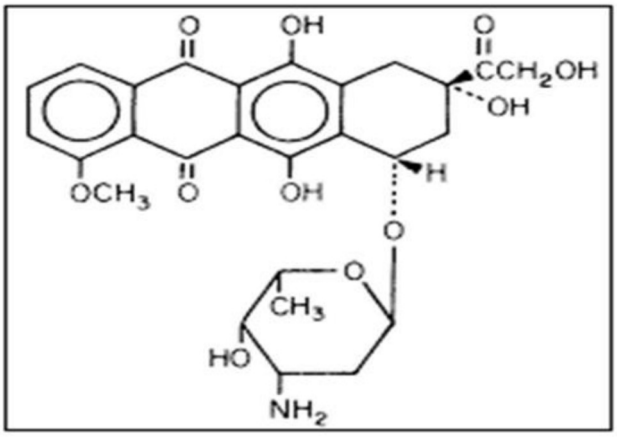

Fig. 1. The structure of the Doxorubicin anti-cancer drug.

influencing the crystallinity, surface area, and other structural characteristics of the SiO_2 nanoparticles. The choice of temperature range and duration could be a deliberate attempt to tailor the properties of the SiO_2 nanoparticles, such as their size, surface area, and porosity, for specific applications, such as drug delivery or catalysis.[27,28]

Adsorption of doxorubicin on SiO_2 NPs

Doxorubicin (DOX) is a commonly adopted anti-cancer drug, which is known for the promising potentials it has in treating solid tumors. Fig. 1 illustrates the structure of the Doxorubicin anti-cancer drug.

Different concentrations of SiO_2 nano-carrier were mixed with 50 ml of DOX aqueous solution (30 ppm). Every combination underwent stirring for 10 minutes at 25 °C at a pH = 6. Next, the isolation of the SiO_2/DOX mixture is obtained via a 10-minutes centrifuging process at a rate of 6000 rpm. The UV-Vis spectro-photometer is utilized to record the concentration of DOX in the super-natant liquids, The Dox adsorption on the surface of silica was determined from the values of optical density of the absorption band at 480 nm using the Eq. (1) as shown in Figs. 2 and 3 below.

$$A_t = (C_o - C_t)\,V/m \quad (1)$$

Where A_t is the adsorption at time t, mol/g, C_o the initial concentration of Dox, mol/l, C_t, the concentration of Dox in a solution at time t, mol/l, V the volume of solution, and m the batch of silica.

The medication is observed to adsorb on the surface of bigger pores and then diffuse into the smaller ones as a result of the interaction between positively charged doxorubicin hydrochloride and negatively

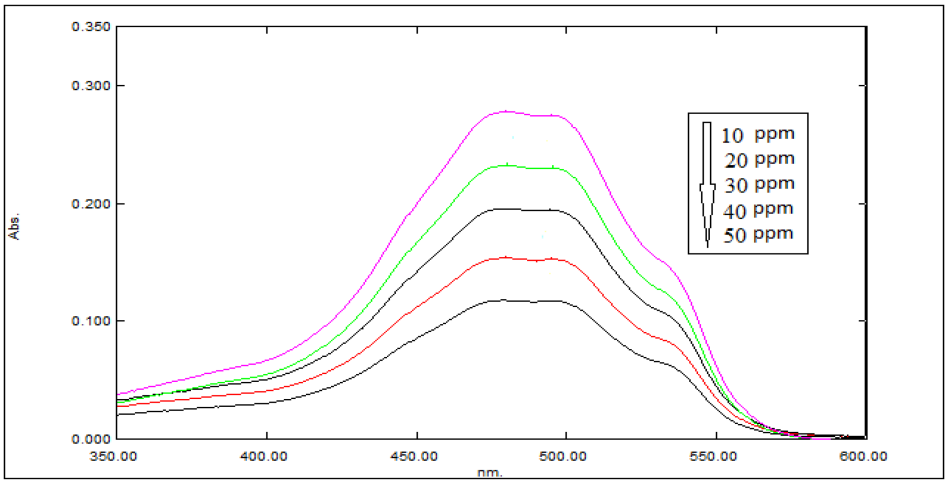

Fig. 2. UV-visible spectra for different concentrations of Doxorubicin.

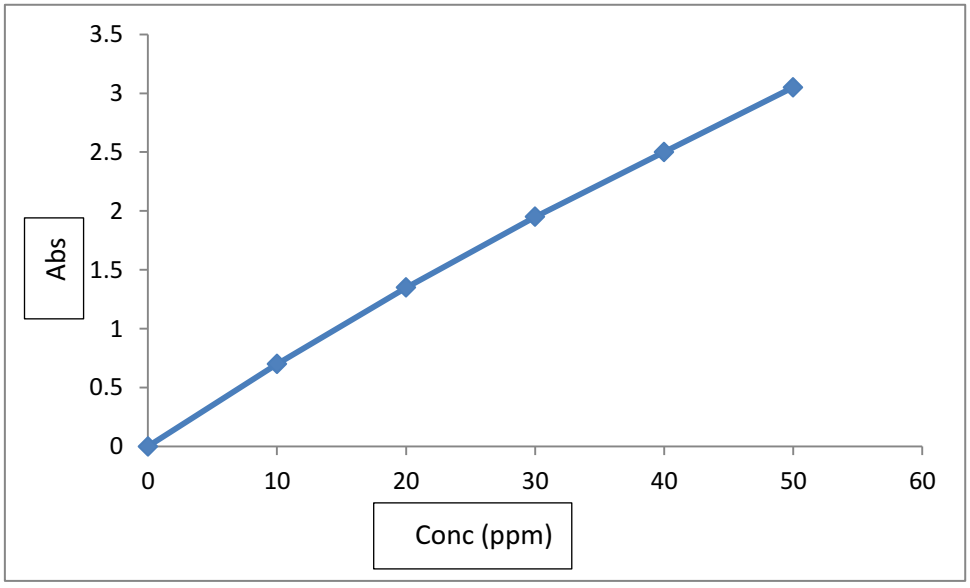

Fig. 3. Calibration curve of Doxorubicin drug at 480 nm.

charged silica centers (pH 6). Additionally, it has been demonstrated that Dox tends to self-aggregate on silica surfaces.[29]

For investigating the isotherms of adsorbing, variations in the temperature of solutions and initial DOX concentrations are applied during the experimental procedures. Eqs. (2) to (4) below are applied for calculating the adsorbing percentage (η) and adsorbing capacity value at equilibrium and time t (qe and qt, mg g^{-1}), respectively:

$$\eta = Co - Ce/Co \times 100\% \quad (2)$$

$$q\,e = (Co - Ce/m)\,.\,V \quad (3)$$

$$q\,t = (Co - Ct/m)\,.\,V \quad (4)$$

Whereby Co, Ce and Ct (mg L^{-1}) represent the concentration of DOX at initial, equilibrium and time t, correspondingly, V (L) represents the solution volume, and m (g) indicates the mass of the applied nano-carriers.

Doxorubicin loading into SiO_2 NPs

To make 30 ppm solutions, doxorubicin was dissolved in distilled water. An amount of (15 mL) of a 10 mg/ml SiO_2 solution was combined with a 5 mL DOX solution. For 24 hours, the combined solution was maintained at 4 °C to get the highest doxorubicin

loading. After being properly rinsed twice with distilled water, the dispersion underwent centrifuging at a speed of 6000 rpm for ten minutes for separating the loaded nano particles. By means of a UV Spectro-photometer having a detection wave length of 480 nm, the amount of pharmaceuticals that are loaded into the nano particles is calculated via deducting the amount of drugs in the super-natant from the amount found within the loading solution.[6]

Characterization techniques

Scanning electron microscopy. The morphology of the resultant formulations was assessed using a scanning electron microscope (SEM; XL30 FEG; Philips). Using Image J software, 300 particles were sized for each created formulation in order to calculate the population's average diameter, standard deviation, and particle size distribution. JEM 2100 used transmission electron microscopy (Carl Zeiss EM900, Germany) to investigate the material's complex internal morphology. Using the X-ray diffract pattern, the crystalline structure, location, and structural properties of MCM-41 with 10 in the range of 0°–100° and scan rate 10 (deg/min) were found. The source of the X-ray radiation was Cu K (=1 0.541oA) (XRD: PW1730: Philips).

Using a (SHIMADZU FT-IR 8400S) in transmission mode, the (FT-IR) infrared spectra under ambient conditions were diluted with KBr, with regions having a resolution of 4 cm^{-1}. Ultraviolet-visible (UV-vis) reflectance spectrum of Dox adsorbed on mesoporous silica was registered in the 350–600 nm spectral range.

Results and discussion

The fourier transform infra-red (FTIR) spectroscopy spectrum

The goal of FTIR characterization is to identify the materials' wave loading pattern. Fig. 4 displays the FTIR spectrum features of the DOX, DOX-loaded SiO_2, and raw as-prepared SiO_2 Fig. 4a, Fig. 4b and Fig. 4c. The analysis findings, as well as the matching of the sample's functional groups to infrared absorption patterns at wavelengths of 465–475 cm^{-1}, 800–870 cm^{-1}, and 3000–4000 cm^{-1}, revealed the absorption patterns of the Si–O functional group, the -OH group of SiO_2, and the O–H group. These absorptions matched the features of the silica's absorption pattern, similar to the findings obtained by.[30–32]

The peaks at 3500 and 2933 cm^{-1} in Fig. 4b and Fig. 4c correspond to hydrogen-bonded N-H stretching and C-H stretching vibrations, respectively. N-H bending vibrations are related to the bands seen at 1620 and 1525 cm^{-1}, whereas C-C vibrations are related to the band seen at 1412 cm^{-1}. Two other distinctive DOX peaks are located at 870 and 805 cm^{-1}, and they signify N-H wagging vibrations.[33] When compared to SiO_2 Fig. 4a, the intensity of the 1414 cm^{-1} peak dramatically increased following adsorption with DOX, Fig. 4c, which may be due to the fact that DOX contains C-C. The distinctive bands at 2930, 1733, 1620, 1285, and 1575 cm^{-1} that are conspicuous for DOX loading SiO_2 relate to DOX. In Fig. 4c, the broadband of about 3700 to 2100 cm^{-1} indicates the vibrating motions of the -OH groups.[34]

X-Ray diffraction (XRD)

The X-ray diffraction patterns of all three SiO_2, DOX and DOX-SiO_2 nanoparticles are illustrated in Fig. 5. It shows the diffraction pattern data for the chemically synthesized SiO_2. Fig. 5a shows the single peak at the position of (2 thata) 21.6°. This silica powder diffraction pattern shows that it was in an amorphous state. The crystallite size of the produced SiO_2 nanoparticles is determined by means of the Debye-Scherrer formula below using the Eq. (5):

$$D = (0.89\,\lambda) / (\beta \cos\theta) \quad (5)$$

It was determined that the sample's average crystallite size is 14.3 nm.

Thus, all subsequently surface-modified materials preserved the seven diffraction peaks that were first seen for DOX Fig. 5b, as well as the 2 theta values at 30.4 o, 35.6 o, 37.3 o, 47.3 o, 56.2 o, 63.5 o, and 68.8 o that were seen on all samples, Fig. 5b and Fig. 5c. This indicates that the DOX's first creation was successful. The XRD patterns of DOX-SiO_2 nano particles after loading with a silica layer resembled those of the SiO_2 nanoparticles.[35–37]

Scanning electron microscopy (SEM)

Fig. 6 in this study illustrates the shape of silica as the outcome of chemical synthesis. It can be seen that the particles were relatively smaller and spherical; however they have a tendency towards an oval shape. The grain boundary was also clearly defined, and the estimated particle size was around 38.00 nm. According to Fig. 6a, the particles resembled a ball and a crystal box.[38]

Fig. 7 below displays the SEM scans of SiO_2, DOX, and SiO_2 that are loaded onto the DOX. It illustrates the dramatic differences in the product surface

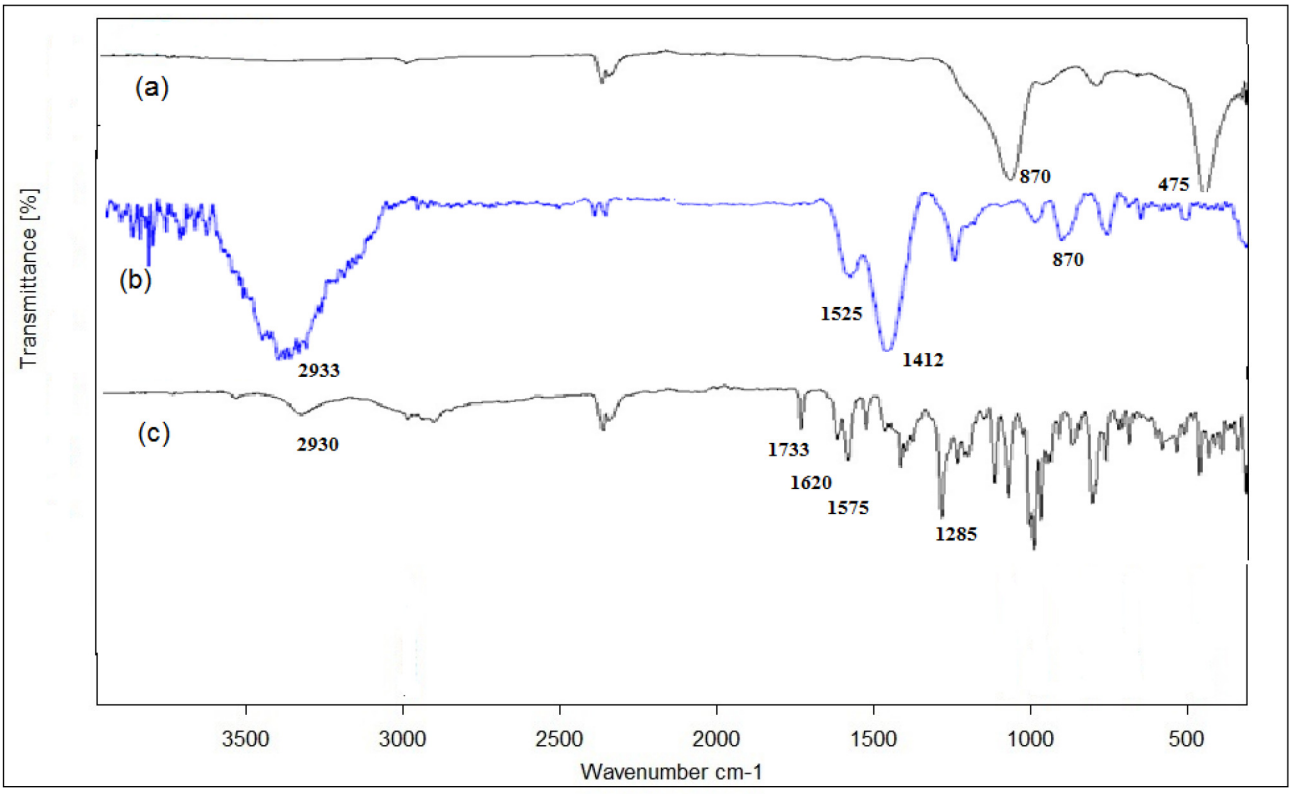

Fig. 4. FTIR spectra for the functionalization of (a) SiO_2 NPs, (b) Doxorubicin, and (c) DOX/SiO_2 nanoparticles after Doxorubicin adsorption.

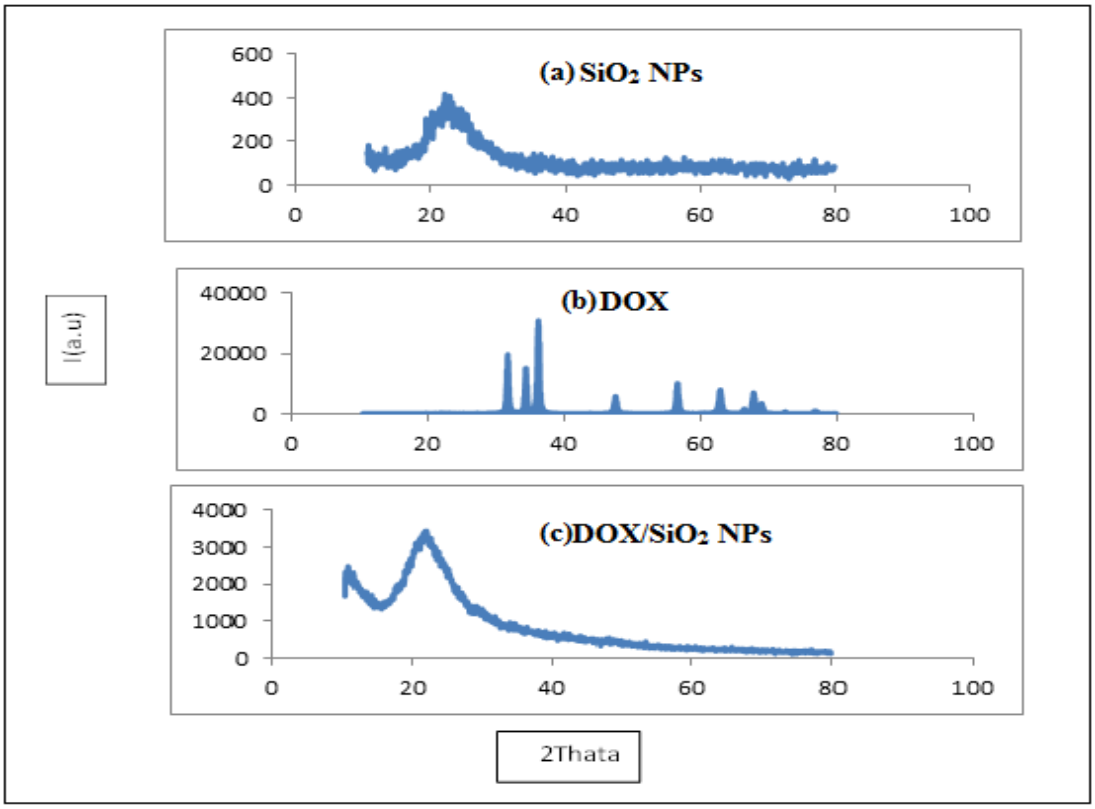

Fig. 5. XRD for (a) SiO_2 NPs, (b) DOX, and (c) Loading DOX-SiO_2 NPs.

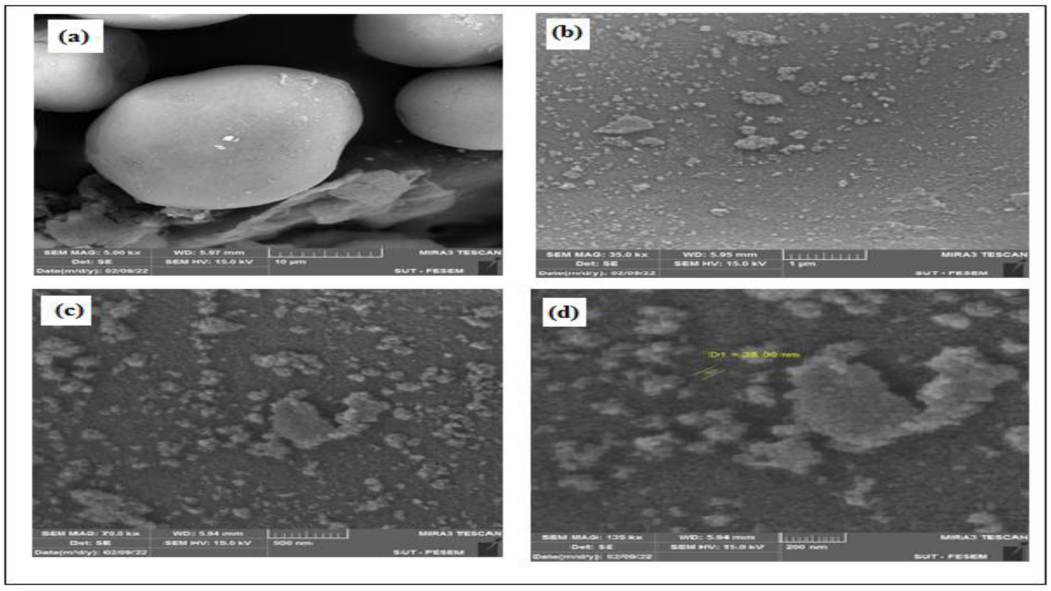

Fig. 6. SEM images of SiO_2 NPs at (a) 10 μm, (b) 1 μm, (c) 200 nm, and (d) 500 nm.

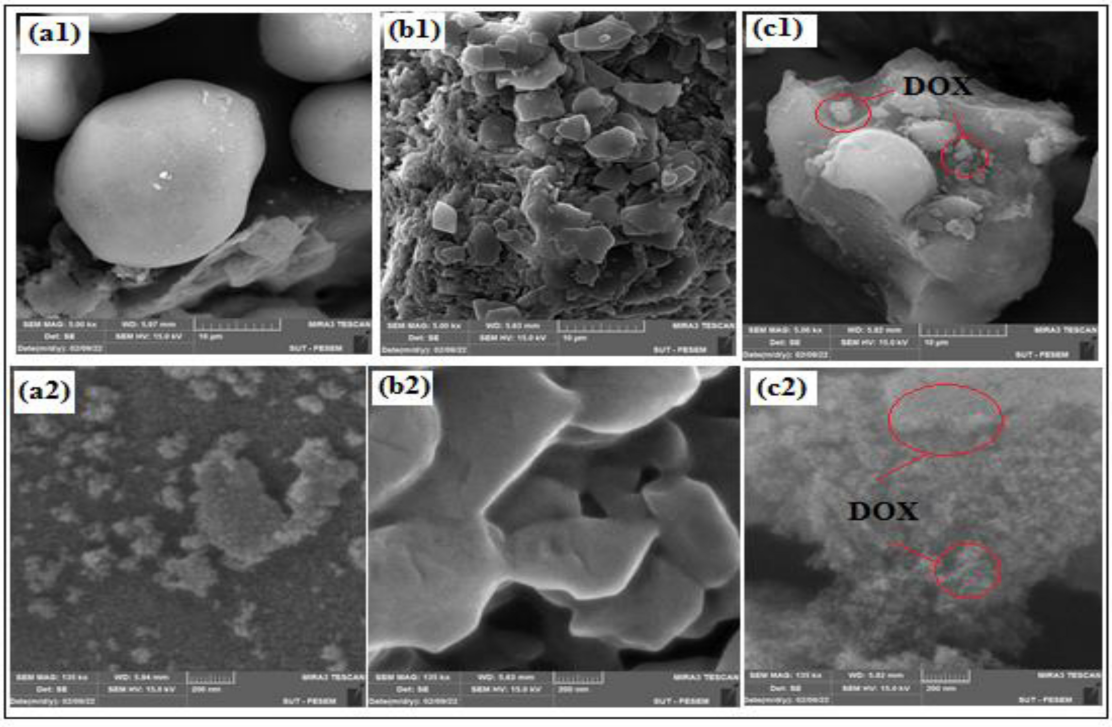

Fig. 7. SEM images of (a1) SiO_2 NPs at (10 μm), (a2) SiO_2 NPs at (200 nm), (b1) DOX at (10 μm), (b2) DOX at (200 nm), (c1) loading DOX-SiO_2 NPs at (10 μm), and (c2) loading DOX-SiO_2 NPs at (200 nm).

morphology before and after being loaded with DOX. According to Fig. 7c1 and Fig. 7c2, the diameter of the bare SiO_2 NPs is 38 nm, which is less than the diameter of the more grain-structured, DOX-loaded SiO_2 particles. Additionally, due to interactions between surface charges, the earlier nanoparticles are agglomerated.[39] After loading with DOX, partially thick and viscous substances are observed, intertwining among grainy nano-particles. The rough surface could be traced back to the loading of DOX particles which subsequently cause the SiO_2 surface to grow.

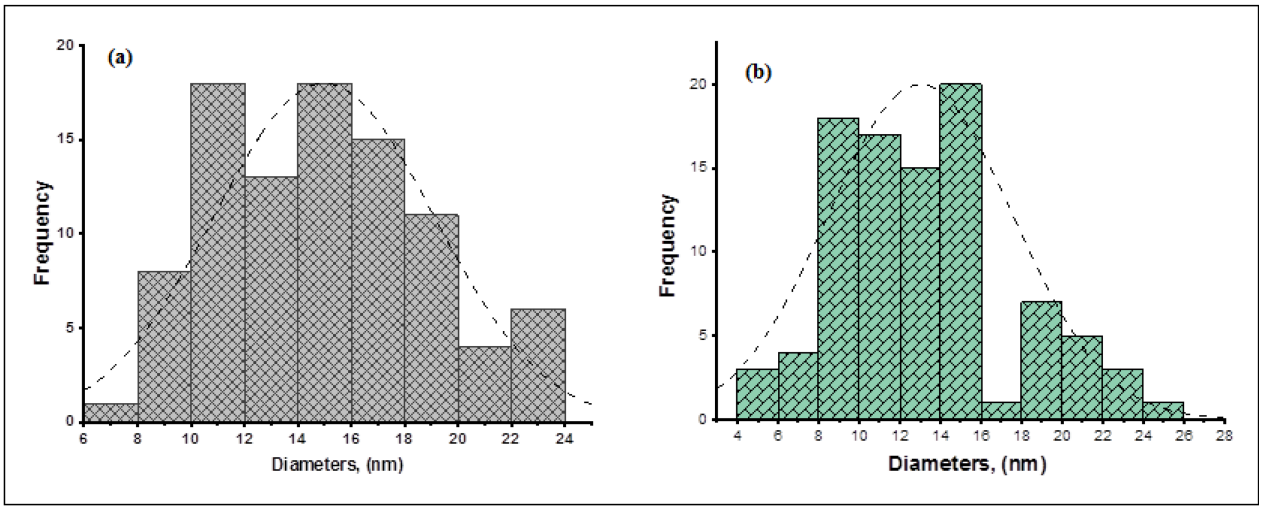

Fig. 8. Histogram displaying the distribution of (a) SiO_2 NPs, and (b) loading DOX-SiO_2 NPs by diameter.

As an additional provision in this part, provide Fig. 8a and Fig. 8b by using the image J software to compute the catalyst. According to SEM zoom 200 nm. The size distribution histograms shown in Fig. 8a, Fig. 8b depicts the average size of the Si NPs, which is found to be 16.5 nm, 15.0 nm for Si NPs and DOX-SiO_2 NPs, respectively. Further, there is a significant increase in the yield of DOX-SiO_2 NPs as compared to SiO_2 NPs.

The adsorption properties of SiO_2-DOX

The initial influences of DOX adsorption over SiO_2 are shown in Fig. 9. A pH of 6.0 in an aqueous solution has essential variables, given its impact on the dynamic destinations of nano-adsorbents and the level of ionization and speciation of the adsorbate. The increasing adsorption productivity along with pH suggests that the surface of functionalized SiO_2 has a more negative charge. It has been noted that DOX adsorption increases along with increases in the adsorbent doses. Also, the increase in ensnarement productivity, with an increase in adsorbent dosage, may be attributed to the accessibility of a large surface area and a more noticeable number of free adsorption sites.

With further increases in adsorbent dosage concentrations, the rate of adsorption does not increase fundamentally. This phenomenon may be due to the fact that both the surface of the adsorbent and the solution concentration of the DOX settle down in order to harmonize with each other. As can be seen in Fig. 9, increasing the SiO_2 concentration from 2 to 10 mg ml^{-1} lead to a corresponding increase in the adsorption percentage. These results may be due to the fact that at high SiO_2 concentrations, the ratio of active sites on the surface of the adsorbent to the overall adsorbate (DOX molecules) concentration is relatively high. On the other hand, when the SiO_2concentration decreases, the numbers of active adsorption sites are not enough to accommodate drug ions.

Kinetics of doxorubicin adsorption

The formulae below which are applied in the fitting of the experimental data can also be used to define the adsorption kinetics as pseudo-first order and pseudo-second order by using the Eqs. (6) and (7), respectively.[26,40]

$$\mathrm{Ln}\,(q_e - q_t) = \ln q_e - k_1 t \tag{6}$$

$$t/q_t = 1/k_2 q_{e2} + t/q_e \tag{7}$$

whereby q_e (mg/g) and q_t (mg/g) represent the DOX adsorbing capacity at a time t (min) and at equilibrium respectively, K_1 min^{-1} represents the equilibrium rate constant of pseudo-first sorption, and K_2 (g/mg · min) represents the pseudo second-order rate constant.

Equations of Lagergren were used to assess the dependences of Dox adsorption on the silica surface on the time of contact for pseudo-first- and pseudo-second-order kinetic models, as shown in Table 1. The linear relationships for solutions with a pH of 6 are plots of $lg(q_e\_q_t)$ (or q_e) versus t Figs. 10 and 11. The adsorption of Dox on silica surface at pH 6.0 can be better explained by a pseudo-second-order kinetic model than by a pseudo-first one, according to comparatively high correlation coefficients. The

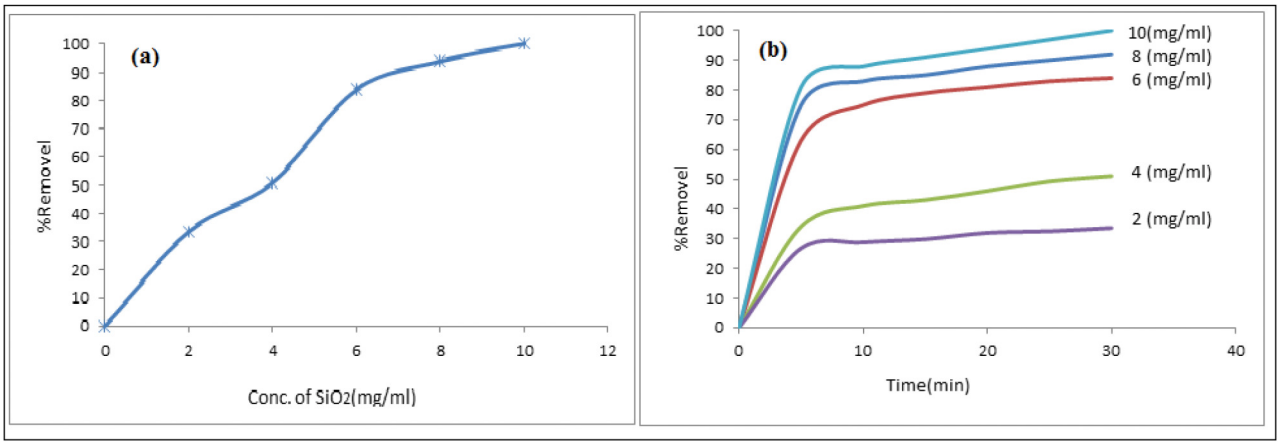

Fig. 9. (a) Effect of SiO_2 concentration on adsorption efficiency, and (b) Effect of contact time on the adsorption of Doxorubicin and its removal by SiO_2: Doxorubicin concentration 10 ppm.

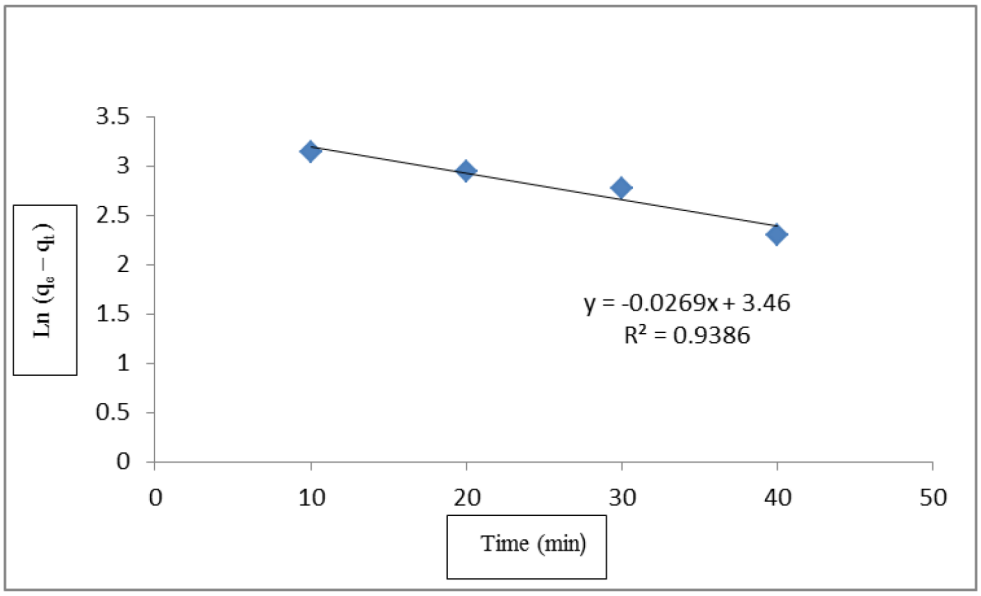

Fig. 10. Plots of the pseudo-first-order kinetic model, for adsorbing 30 ppm Doxorubicin onto SiO_2, at 25 °C, with adsorbent dose of 10 mg/ml and pH of 6.

slope and intercept of linear plots were used to compute kinetic rate constants and the quantities of Dox adsorbed from phosphate buffer solutions at equilibrium Figs. 10 and 11. These adsorption isotherms can be used to understand the mechanism of interaction between the adsorbent and the adsorbate. Adsorption and release behavior are crucial for the effective use of any anti-cancer medication; for this reason, the substance now absorbed with DOX was examined using this method.

The kinetics research was fitted using the experimental data that was acquired. As shown in Table 1. illustrates how the pseudo-second order adsorption represents the optimal match for DOX adsorption.

Table 1. Kinetics factors for pseudo-first and -second order models for the DOX adsorption on SiO_2.

Pseudo first order		Pseudo second order	
K_1 (min^{-1})	R^2	K_2 (min^{-1})	R^2
0.007	0.9386	0.0122	0.9477

Adsorption isotherms

The Langmuir and Freundlich isotherm models have been used in analyzing the equilibrium data. They could be illustrated by means of Eqs. (8) and (9) below, respectively. [41]

$$\text{Langmuir } 1/q_e = 1/q_m + 1/K_L q_m C_e \quad (8)$$

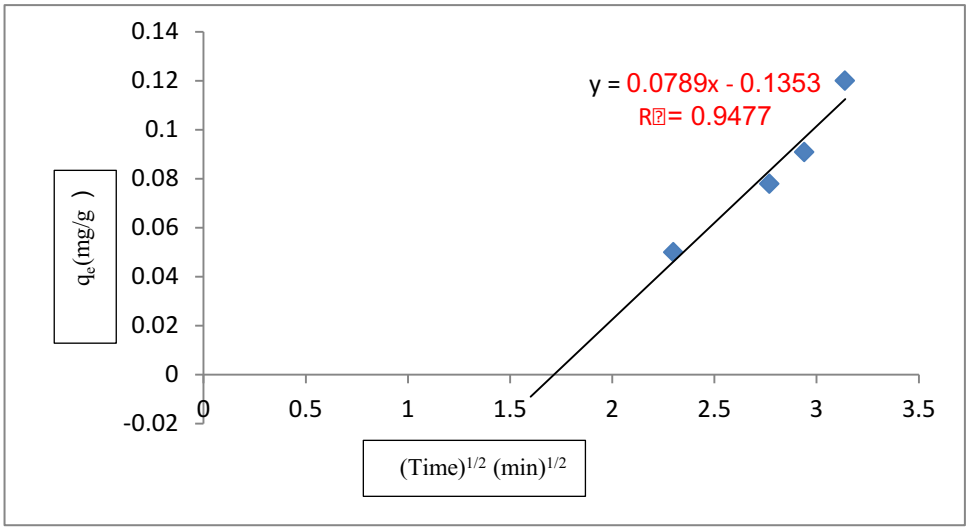

Fig. 11. Plots of the pseudo-second-order kinetic model, for adsorbing 30 ppm Doxorubicin onto SiO_2, at 25 °C, with adsorbent dose of 10 mg/ml and pH of 6.

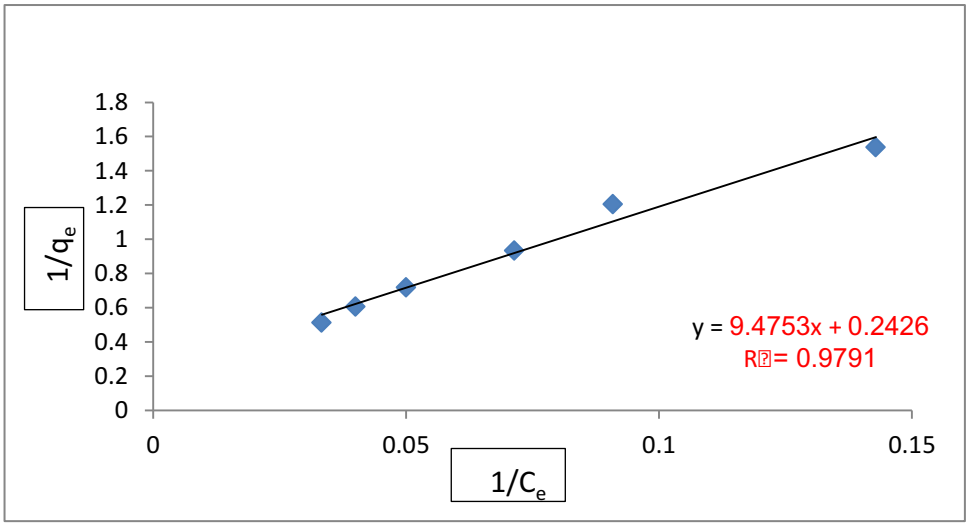

Fig. 12. Linear Langmuir adsorption isotherms for Doxorubicin adsorption by SiO_2.

$$\text{Freundlich } \log q_e = \log K_F + 1/n \log C_e \quad (9)$$

where by C_e (mg/L) represents the concentrations of the DOX solution in equilibrium after reaction, q_e (mg/g) represents the adsorbing capacity in equilibrium, q_m (mg/g) represents the maximal adsorbing capacity, KL (L/mg) represents the Langmuir adsorbing constant, 1/n and K_F (mg/$L^{1/1-n}$ g) represents the intensity of the adsorbing isotherm constants and adsorbing capacities, respectively.

These adsorption isotherms can be applied for comprehending the mechanism according to which the adsorbents and adsorbates interact. Adsorption and release behavior are crucial for the effective application of any anticancer medication. Therefore, the current material absorbed onto DOX is tested using this method. As a statistical indicator, the linear correlation coefficient (R^2) value ranges from 0 to 1. It displays the level of correlation between several factors. There is no correlation between the projected values and the experimental data whenever the correlation coefficient appears to be relatively lower, maybe closer to zero. On the other hand, a value of R^2 that is equal to or nearly equal to 1 indicates excellent fitting.[42,43]

The experimental data utilized in the calculation of the kinetic and thermodynamic features were all obtained from Figs. 12 and 13. The values of R^2 for the Freundlich and Langmuir model were 0.9931 and 0.9731, respectively. This creates the indication that

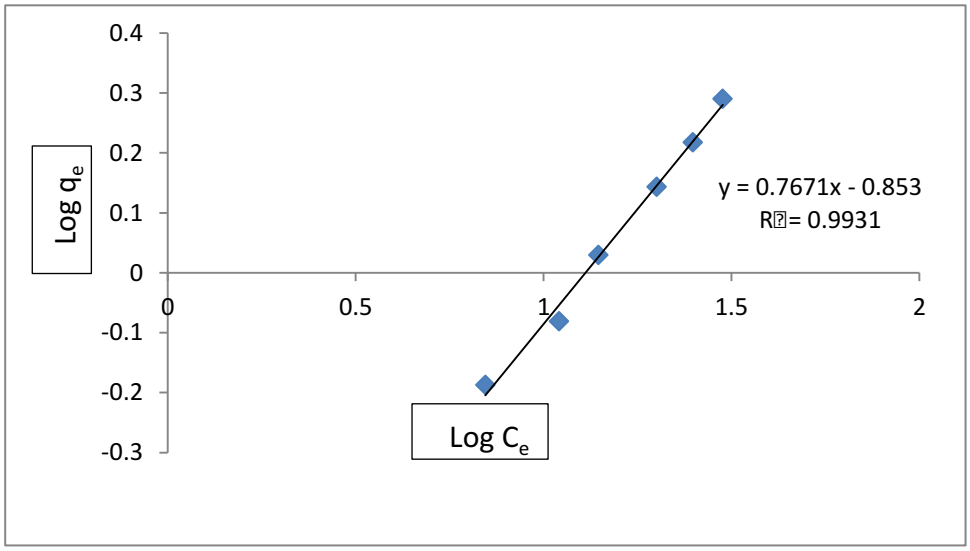

Fig. 13. Linear Freundlich adsorption isotherms for Doxorubicin adsorption by SiO_2.

the Freundlich isotherm is a more suitable fit for the experimental data in comparison with the Langmuir model. The value of n = 2.4188, qm = 70.942 mg/g, K_L = 0.5872 L/mg and K_F = 26.9720 mg/g were calculated, indicating that the DOX adsorption took place in form of multi-layer adsorbing onto the surface of SiO_2. Furthermore, the value of 1/n implies that the DOX adsorption is dominantly chemical.

Conclusion

The present study examined the loading of Doxorubicin (DOX) onto modified SiO_2 using single-vessel hydrogen bonding reactions. It was observed that the SiO_2 surface modification provides an opportunity to realize a drug delivery system sensitive to catalysts. The formation and properties of the nanoformation were investigated using microscopy and spectroscopy. This study showed that DOX is efficiently loaded onto nanostructures and exhibits lower release in the physiological environment in comparison with unmodified nano-particles when found in acidic conditions. The resulting data implies that the prepared nanostructures are promising nano-carriers for the purpose of drug anti- cancer. For the DOX delivery system, a unique carrier is created with excellent anti-cancer activity and pH-triggered release, kinetics of Dox adsorption on silica surface at pH 6.0 agrees with the kinetic model of pseudo-second order, which is found to have a considerable significance in the treatment of cancer. The adsorption efficiency of the nanoparticles reached to a maximum of 100% for the drug. These systems also offer controlled release therapy and the ability to administer drugs to particular regions. By delivering the medication in a targeted and sustained manner, the toxicity associated with the treatment is reduced, and patients comply with fewer doses. In addition to improving diagnostic tests, nanotechnology has shown promise in the treatment of numerous diseases, including AIDS, cancer, and other conditions. In light of the outcomes, we suggest fostering a productive methodology for creating transferrin-formed Fe_3O_4/SiO_2 nanoparticles, with high DOX loading, for designated anticancer medication conveyance and concentrating on their construction and biomedical properties.

Acknowledgment

The authors state their truthful appreciations to College of Pharmacy, University in Babylon-Iraq for the financial support of this study.

Authors' declaration

- Conflicts of Interest: None.
- We hereby confirm that all the Figures and Tables in the manuscript are ours. Furthermore, any Figures and images, that are not ours, have been included with the necessary permission for republication, which is attached to the manuscript.
- No animal studies are present in the manuscript.
- No human studies are present in the manuscript.
- Ethical Clearance: The project was approved by the local ethical committee at University of Babylon.

Authors' contribution statement

All authors contributed to the completion of this work. N.H.A. and F.G.G. were responsible for preparing the samples and performing the tests. A.H.H. wrote the manuscript, performed the analysis of the data and evaluated the information.

References

1. Lin YQ, Zhang J, Liu SJ, Ye H. Doxorubicin loaded silica nanoparticles with dual modification as a tumor-targeted drug delivery system for colon cancer therapy. J Nanosci Nanotechnol. 2018;18(4):2330–2336. https://doi.org/10.1166/jnn.2018.14391.
2. Shalaby TI, El-Refaie WM, El-Din R S, Hassanein SA. Smart ultrasound-triggered doxorubicin-loaded nanoliposomes with improved therapeutic response: a comparative study. J Pharm Sci. 2020;109(8):2567–2576. https://doi.org/10.1016/j.xphs.2020.05.008.
3. Nguyen TN, Nguyen TT, Nghiem TH, Nguyen DT, Tran TT, Vu D, *et al.* Optical properties of doxorubicin hydrochloride load and release on silica nanoparticle platform. Molecules. 2021;26(13):3968. https://doi.org/10.3390/molecules26133968.
4. Chen Y, Shi S, Dai Y. Research progress of therapeutic drugs for doxorubicin-induced cardiomyopathy. Bio medi Pharm. 2022;156:113903. https://doi.org/10.1016/j.biopha.2022.113903 .
5. Corremans R, Adão R, De Keulenaer GW, Leite Moreira AF, Brás-Silva C. Update on pathophysiology and preventive strategies of anthracycline-induced cardiotoxicity. Clini Pharm Phys. 2019;46(3):204–215. https://doi.org/10.1111/1440-1681.13036.
6. Wence D, Lin G. Immobilized transferrin Fe_3O_4@ SiO_2 nanoparticle with high doxorubicin loading for dual-targeted tumor drug delivery. Int J nanomedicine. 2013;4631–4639. https://doi.org/10.2147/IJN.S51745.
7. Munawar T, Nadeem MS, Rehman MN, Mukhtar M, Iqbal F. Sol–gel synthesis of $Cu_{0.9}Zn_{0.05}M_{0.05}O$ (M = Cr, Co, Cd) nanocrystals for removal of pollutant dyes and bacterial inactivation. J Mater Sci Mater. 2012;32(11):14437–14455. https://doi.org/10.1016/j.apt.2023.104061.
8. Maha AY, Baker FA. Synthesis, characterization and anticancer activity of chitosan schiff base/PVP gold nano composite in treating esophageal cancer cell line. Baghdad Sci J. 2024;21(1):0095–0095. https://dx.doi.org/10.21123/bsj.2023.7911.
9. Rafik ST, Vaidya JS, MacRobert AJ, Yaghini E. Organic nanodelivery systems as a new platform in the management of breast cancer: a comprehensive review from preclinical to clinical studies. J Clin Med. 2023;12(7):2648. https://doi.org/10.3390/jcm12072648.
10. Rabbani AW, Naz G, Berdimurodov E, Lal B, Sailauovna AB, Bandegharaei AH. Visible-light-driven photocatalytic properties of copper (I) oxide (Cu_2O) and its graphene-based nanocomposites. Baghdad Sci J. 2023;20(3):1064–1064. https://dx.doi.org/10.21123/bsj.2023.8476.
11. Munawar T, Nadeem MS, Mukhtar F, Manzoor S, Ashiq MN, Batool S. Multifunctional dual Z-scheme heterostructured Sm_2O_3-WO_3-La_2O_3 nanocomposite: enhanced electrochemical, photocatalytic, and antibacterial properties. Adv Powder Technol. 2023;34(7):104061. https://doi.org/10.1007/s10854-021-06003-4.
12. Gao Y, Gao D, Shen J, Wang Q. A review of mesoporous silica nanoparticle delivery systems in chemo-based combination cancer therapies. J Front chem. 2020;8:598722. https://doi.org/10.3389/fchem.2020.598722.
13. Oliveira LF, Bouchmella K, Goncalves KD, Bettini J, Kobarg J, Cardoso MB. Functionalized silica nanoparticles as an alternative platform for targeted drug-delivery of water insoluble drugs. Langmuir. 2016;32(13):3217–3225. https://doi.org/10.1021/acs.langmuir.6b00214.
14. Schultz HB, Kovalainen M, Peressin KF, Thomas N, Prestidge CA. Supersaturated silica-lipid hybrid oral drug delivery systems: balancing drug loading and in vivo performance. J Pharmacol Exp Ther. 2019;370(3):742–750. https://doi.org/10.1124/jpet.118.254466.
15. Patsos G, André S, Roeckel N, Gromes R, Gebert J, Kopitz, J, Gabius HJ. Compensation of loss of protein function in microsatellite-unstable colon cancer cells (HCT116): a gene-dependent effect on the cell surface glycan profile. Glycobiology. 2009;19(7):726–734. https://doi.org/10.1093/glycob/cwp040.
16. Habeeb SA, Hammadi AH, Abed D, Al-Jibouri LF. Green synthesis of metronidazole or clindamycin-loaded hexagonal zinc oxide nanoparticles from Ziziphus extracts and its antibacterial activity. Pharmacia. 2020;69(3):855–864. https://doi.org/10.3897/pharmacia.69.e91057.
17. Trushina DB, Sapach AY, Burachevskaia OA, Medvedev PV, Khmelenin DN, Borodina TN, *et al.* Doxorubicin-loaded core–shell UiO-66@ SiO_2 metal–organic frameworks for targeted cellular uptake and cancer treatment. Pharmaceutics. 2022;14(7):1325. https://doi.org/10.3390/pharmaceutics14071325.
18. Li X, Zhang X, Zhao Y, Sun L. Fabrication of biodegradable Mn-doped mesoporous silica nanoparticles for pH/redox dual response drug delivery. J Inorg Bio Chem. 2020;202:110887. https://doi.org/10.1016/j.jinorgbio.2019.110887.
19. Nassar MY, El-Salhy HI, El-Shiwiny WH, Abdelaziz G, El-Shiekh R. Composite nanoarchitectonics of magnetic silicon dioxide-modified chitosan for doxorubicin delivery and in vitro cytotoxicity assay. J Inorg Organomet Polym Mater. 2023;33(1):237–253. https://doi.org/10.1007/s10904-022-02498-4.
20. Liu RX, Hao XJ, Zhang HJ, Zhang L, Gui XJ, Lin Z, *et al.* A rapid identification of authenticity and specifications of Chinese medicine Fritillariae Cirrhosae Bulbus based on E-eye technology. J Chin Mater Medica. 2020;45(14):3441–3451. https://doi.org/10.19540/j.cnki.cjcmm.20200601.301.
21. Leila V, Parviz R, Fatemeh D. Cladosporium protease/doxorubicin decorated Fe_3O_4@ SiO_2 nanocomposite: an efficient nanoparticle for drug delivery and combating breast cancer. J Drug Deliv Sci Technol. 2023;80:104144. https://doi.org/10.1016/j.jddst.2022.104144.
22. Ji L, Zheng H, Li S, Li D, Gao Q, Yang J. Doxorubicin-loaded Mn-doped SiO_2 nanospheres coated with carboxymethyl chitosan: fabrication, characterization, and in vitro evaluation. J Chem Res. 2022;46(4):114617. https://doi.org/10.1177/17475198221114617.
23. Kovrigina E, Poletaeva Y, Zheng Y, Chubarov A, Dmitrienko E. Nylon-6-coated doxorubicin-loaded magnetic nanoparticles and nanocapsules for cancer treatment. Magnetochemistry. 2023;9(4):106. https://doi.org/10.3390/magnetochemistry9040106.

24. Bosetti R, Vereeck L. The impact of effective patents on future innovations in nanomedicine. Pharm Pat Anal. 2012;1(1):37–43. https://doi.org/10.4155/ppa.11.4.
25. Miguel G, Miguel M, María V. Mesoporous silica nanoparticles for the treatment of complex bone diseases: Bone cancer, bone infection and osteoporosis. Pharmaceutics. 2020;12(1):83. https://doi.org/10.3390/pharmaceutics12010083.
26. Yang S, Li N, Chen D, Qi X, Xu Y, Xu Y, *et al.* Visible-light degradable polymer coated hollow mesoporous silica nanoparticles for controlled drug release and cell imaging. J Mater Chem B, 2013;1(36):4628–4636. https://doi.org/10.1039/C3TB20609B.
27. Noor HY, Ahmed ES. Green nanocomposites: Magical solution for environmental pollution problems. Advances in Nanocomposite Materials for Environmental and Energy Harvesting Applications. Springer International Publishing 2022;389–417. https://doi.org/10.1007/978-3-030-94319-6_13.
28. Hendry IE. Nanomedicine with its multitasking applications: a view for better health. IJHMCR, 2017;2(2):353–357. https://doi.org/10.22301/IJHMCR.2528-3189.353.
29. Ranathunge TA, Karunaratne DG, Rajapakse RM, Watkins DL. Doxorubicin loaded magnesium oxide nanoflakes as pH dependent carriers for simultaneous treatment of cancer and hypomagnesemia. Nanomaterials. 2019;9(2):2–11. https://doi.org/10.3390/nano9020208.
30. Supardi ZA, Nisa Z, Kusumawati DH, Putri NP, Taufiq A, Hidayat N. Phase transition of SiO_2 nanoparticles prepared from natural sand: the calcination temperature effect. J Phys: Conf Ser. 2018;012025. https://doi.org/.1088/1742-6596/1093/1/012025.
31. Nariyal RK, Kothari P, Bisht B. FTIR measurements of SiO_2 glass prepared by sol-gel technique. Chem Sci Trans. 2014;3(3):1064–1066. https://doi.org/10.7598/cst2014.816.
32. Zainuri M. Synthesis of SiO nanopowders containing quartz and cristobalite phases from silica sands. Mater Sci-Poland. 2015;33(1):47–55. https://doi.org/10.1515/msp-2015-0008.
33. Ebadi M, Buskaran K, Bullo S, Hussein MZ, Fakurazi S, Pastorin G. Drug delivery system based on magnetic iron oxide nanoparticles coated with (polyvinyl alcohol-zinc/aluminium-layered double hydroxide-sorafenib). Alex Eng J. 2021;60(1):733–747. https://doi.org/10.1016/j.aej.2020.09.061.
34. Cai W, Guo M, Weng X, Zhang W, Chen Z. Adsorption of doxorubicin hydrochloride on glutaric anhydride functionalized Fe3O4@ SiO_2 magnetic nanoparticles. Mater Sci Eng: C. 2019;98:65–73. https://doi.org/10.1016/j.msec.2018.12.145.
35. Hammadi AH, Assi LN, Hussien, FH. Drug loading on carbon nanotubes synthesized by flame fragments deposition technique. Sys Rev Pharm. 2020;11(3). http://dx.doi.org/10.5530/srp.2019.2.04.
36. Ali AS, Fadhil JF, Fulla AA. Green synthesis of silver nanoparticles using aqueous extract of typha domingensis pers. Pollen (qurraid) and evaluate its antibacterial activity. Baghdad Sci J. 2024;21(1):0028–0028. https://dx.doi.org/10.21123/bsj.2023.
37. Cai, W, Guo M, Weng X, Zhang W, Owens G, Chen Z. Modified green synthesis of Fe_3O_4@ SiO_2 nanoparticles for pH responsive drug release. Mater Sci Eng: C. 2020;112:110900. https://doi.org/10.1016/j.msec.2020.110900.
38. Purcar V, Rădiţoiu V, Rădiţoiu A, Manea R, Raduly FM. Ispas GC, *et al.* Preparation and characterization of some sol-gel modified silica coatings deposited on polyvinyl chloride (PVC) substrates. Coatings. 2020;11(1):2–13. https://doi.org/10.3390/coatings11010011.
39. Nguyen TN, Nguyen TT, Nghiem TH, Nguyen DT, Tran, T. T, Vu D, *et al.* Optical properties of doxorubicin hydrochloride load and release on silica nanoparticle platform. Molecules. 2021;26(13):3968. https://doi.org/10.3390/molecules26133968.
40. Nadiia VR, Lyudmila AB, Marina OD. Adsorption of antitumor antibiotic doxorubicin on MCM-41-type silica surface. Adsorpt Sci Technol. 2017;35(1):86–101. https://doi.org/10.1177/0263617416669504.
41. Munawar T, Yasmeen S, Hussain F, Mahmood K, Hussain A, Asghar M, *et al.* Synthesis of novel heterostructured ZnO-CdO-CuO nanocomposite: characterization and enhanced sunlight driven photocatalytic activity. Mater Chem Phys. 2020;249:122983. https://doi.org/10.1016/j.matchemphys.2020.122983.
42. Lei Y, Yong ML. The adsorption mechanism of anionic and cationic dyes by Jerusalem artichoke stalk-based mesoporous activated carbon. J Environ Chem Eng. 2014;2(1):220–229. https://doi.org/10.1016/j.jece.2013.12.016.
43. Hania A, Hazim Q, Muftah H. Comparative study between adsorption and membrane technologies for the removal of mercury. Sep Purif. Technol. 2021;257:117833. https://doi.org/10.1016/j.seppur.2020.117833.

تحضير وتشخيص وامتزاز كلوريد دكسوربيسين على الجسيمات النانوية لثاني اوكسيد السليكا لتوصيل الدواء

اسماء هاشم حمادي[1]، نور هادي عيسى[2]، فاطمة الزهراء جبار جاسم[1]

[1]قسم صيدلانيات، كلية صيدلة، جامعة بابل، الحلة، العراق.
[2]قسم علوم سريرية ومختبرية، كلية صيدلة، جامعة بابل، الحلة، العراق.

الخلاصة

في هذه الدراسة، تم استخدام رباعي إيثيل أورثوسيليكات (TEOS) والبولي إيثيلين جلايكول 5% وحمض الهيدروكلوريك 0.001 نورمالي لإنشاء جسيمات السيليكا النانوية كيميائيا (SiO_2 NPs). تم تصنيع جسيمات السيليكا النانوية المحملة بدوكسوروبيسين (DOX) (DOX / SiO_2)، والتي يتم تطبيقها بشكل شائع كجزء من أنظمة توصيل الأدوية في علاج السرطان ، باستخدام طريقة سول جل. تمت دراسة التشكل والمحتوى السطحي للجسيمات النانوية المحملة ب DOX / السيليكا المنتجة باستخدام تقنيات مختلفة بما في ذلك حيود الأشعة السينية (XRD)، والمجهر الإلكتروني الماسح (SEM)، وطيف التحليل الطيفي بالأشعة تحت الحمراء (FTIR). يبلغ قطر DOX / SiO_2 المركب 38 نانومتر. يتبع الامتزاز متساوي الحرارة متساوي الحرارة hcildnuerF وحركية الامتزاز المناسبة للترتيب الثاني الزائف. كانت قيم R2 لنماذج Freundlich و Langmuir 0.9931 و 0.9731، على التوالي ، مما يدل على أن متساوي الحرارة Freundlich يميل إلى أن يكون أكثر ملاءمة مع البيانات التجريبية مقارنة بنموذج Langmuir. تهدف هذه الدراسة إلى استخدام تقنية النانو في توصيل الدواء، وبالتالي التغلب على عيوب DDS الشائعة.

الكلمات المفتاحية: امتزاز، دكسوربسين، توصيل الدوائي، جزيئات اوكسيد السليكا النانوي، طريقة السول جل.